PROCEEDINGS, 44th Workshop on Geothermal Reservoir Engineering
Stanford University, Stanford, California, February 11-13, 2019
SGP-TR-214

Anisotropic Elastic-Waveform Inversion and Least-Squares Reverse-Time Migration of CASSM Data for Experiment I of the EGS Collab Project

Wenyong Pan[1], Lianjie Huang[1], Kai Gao[1], Jonathan Ajo-Franklin[2], Timothy J. Kneafsey[2], and EGS Collab Tem[*]

[1]Los Alamos National Laboratory, Geophysics Group, MS D452, Los Alamos, NM 87545, USA

[2]Lawrence Berkeley National Laboratory, 1 Cyclotron Road, Berkeley CA 94720, USA

wenyongp@lanl.gov; ljh@lanl.gov

Keywords: Anisotropic, enhanced geothermal systems, EGS Collab project, elastic-waveform inversion, fracture, least-squares reverse-time migration, stimulation

ABSTRACT

The EGS Collab project, supported by the U.S. Department of Energy's Geothermal Technologies Office, is conducting field experiments at the Sanford Underground Research Facility (SURF) site to study the fracture creation using stimulation. A multi-level continuous active source seismic monitoring (ML-CASSM) system is used to monitor the fracture creation. Four fracture-parallel and two orthogonal wells with hydrophones and accelerometers are used to acquire active and passive seismic data during the field experiments. We apply 3D anisotropic elastic-waveform inversion to the CASSM data to obtain an elastic model for the experimental region. Using the inverted elastic model, we apply 3D anisotropic, acoustic least-squares reverse-time migration to the CASSM data to produce a high-resolution image. Our preliminary result of anisotropic elastic-waveform inversion shows the rock is anisotropic and heterogeneous. Our least-squares reverse-time migration detects the stimulation-created fracture, and the image shows that the fracture plane may not be isotropic either.

1. INTRODUCTION

Fracture characterization is essential for geothermal energy exploration and production. The EGS Collab (Stimulation Investigations for Geothermal Modeling Analysis and Validation) project, supported by the U.S. DOE Geothermal Technologies Office (GTO), is conducting field experiments at the Sanford Underground Research Facility (SURF) site to study fracture creation and imaging (Kneafsey et al., 2019). The first experiment was conducted from a drift located approximately 1.5 km below the surface at Lead, South Dakota, in May, 2018. The purpose of the experiment is to understand the hydraulic stimulations in crystalline rock for enhanced geothermal system (EGS) production.

Monitoring the fracture creation using geophysical methods is one important component of the EGS Collab project. A multi-level continuous active source seismic monitoring (ML-CASSM) system (Ajo-Franklin et al., 2011) is used to monitor fractures created by hydraulic stimulations. Four fracture-parallel boreholes and two fracture-orthogonal boreholes are used to acquire active and passive seismic data during the experiment. Two cemented hydrophone strings with 12 sensors at 1.75 m spacing accompanied by 18 3-C accelerometers were deployed in the six monitoring boreholes. Another four 3-C geophones were deployed in sub-vertical jackleg-drilled holes. The CASSM data consisting of 96 channels were recorded continuously for two months using a novel dual recording system.

Stimulations tests were performed on several notched locations. The notch at 164 ft depth was stimulated several times to increase the hydraulic fracture size. The first test was carried out on 05/22/2018. The stimulation lasted about 10.5 minutes at pressures of 23.1 to 25.5 MPa (3350 to 3700 psi) with a total injection volume of 2.1 liters and an injection rate of ~200 ml/min. On 05/23/2018, sufficient fluid (23.5 liters) was injected to extend the fracture size with a maximum pressure of 26.33 MPa (3819 psi). On 05/24/2018, the injection was continued for fracture extension, which made the connections to boreholes E1-OT and E1-P. We use the data recorded on 05/24/2018 for seismic inversion and imaging for fracture detection.

Reverse-time migration (RTM) is a powerful technique for imaging complex subsurface structures. However, the quality of an RTM image depends on the accuracy of the velocity model used. Furthermore, RTM suffers from low-wavenumber artifacts and produces

[*] J. Ajo-Franklin, S.J. Bauer, T. Baumgartner, K. Beckers, D. Blankenship, A. Bonneville, L. Boyd, S.T. Brown, J.A. Burghardt, T. Chen, Y. Chen, K. Condon, P.J. Cook, P.F. Dobson, T. Doe, C.A. Doughty, D. Elsworth, J. Feldman, A. Foris, L.P. Frash, Z. Frone, P. Fu, K. Gao, A. Ghassemi, H. Gudmundsdottir, Y. Guglielmi, G. Guthrie, B. Haimson, A. Hawkins, J. Heise, C.G. Herrick, M. Horn, R.N. Horne, J. Horner, M. Hu, H. Huang, L. Huang, K. Im, M. Ingraham, T.C. Johnson, B. Johnston, S. Karra, K. Kim, D.K. King, T. Kneafsey, H. Knox, J. Knox, D. Kumar, K. Kutun, M. Lee, K. Li, R. Lopez, M. Maceira, N. Makedonska, C. Marone, E. Mattson, M.W. McClure, J. McLennan, T. McLing, R.J. Mellors, E. Metcalfe, J. Miskimins, J.P. Morris, S. Nakagawa, G. Neupane, G. Newman, A. Nieto, C.M. Oldenburg, W. Pan, R. Pawar, P. Petrov, B. Pietzyk, R. Podgorney, Y. Polsky, S. Porse, S. Richard, B.Q. Roberts, M. Robertson, W. Roggenthen, J. Rutqvist, D. Rynders, H. Santos-Villalobos, M. Schoenball, P. Schwering, V. Sesetty, A. Singh, M.M. Smith, H. Sone, C.E. Strickland, J. Su, C. Ulrich, N. Uzunlar, A. Vachaparampil, C.A. Valladao, W. Vandermeer, G. Vandine, D. Vardiman, V.R. Vermeul, J.L. Wagoner, H.F. Wang, J. Weers, J. White, M.D. White, P. Winterfeld, T. Wood, H. Wu, Y.S. Wu, Y. Wu, Y. Zhang, Y.Q. Zhang, J. Zhou, Q. Zhou, M.D. Zoback

blurred image. Elastic-waveform inversion (EWI) estimates the model parameters using the entire waveform information, and can recover small-scale structures and produce high-resolution velocity models.

In this study, we apply our newly developed anisotropic elastic-waveform inversion (AEWI) to the CASSM data recorded on 05/24/2018 for obtaining elastic parameters. Using the inverted elastic parameters, we apply anisotropic, acoustic least-squares reverse-time migration (LSRTM) to obtain a high-resolution migration image. From the LSRTM image, we can clearly identify the created facture, which intersects the injection well E1-I and matches the location of the notch at 164.4 ft depth.

The paper is organized as follows. We first review the forward modeling problem in general anisotropic-elastic media. Then, we describe our AWEI method and anisotropic LSRTM. In CASSM data application section, we introduce the ML-CASSM system for data acquisition, illustrate the CASSM data used for inversion and imaging, and present the preliminary results obtained using AEWI and anisotropic LSRTM.

2. METHODOLOGY

2.1 Anisotropic Elastic-Waveform Inversion with Total Generalized P-Variation Regularization

To estimate subsurface anisotropy and velocity properties, we use anisotropic elastic-waveform inversion (AEWI) to invert for elastic constants C_{ij} (i and j : $1,2,...,6$). Wave propagation in general anisotropic media is simulated by solving the following first-order velocity-stress partial differential equations:

$$\frac{\partial v}{\partial t} = \rho^{-1}\Lambda\sigma, \tag{1}$$

$$\frac{\partial \sigma}{\partial t} = C\Lambda^{T}v, \tag{2}$$

where ρ is the mass density, $C = C_{ij}$ is the elastic stiffness tensor, $v = \left(v_x, v_y, v_z\right)$ is the particle velocity field, Λ is the partial differential operator, $\sigma = \left(\sigma_{xx}, \sigma_{yy}, \sigma_{zz}, \sigma_{yz}, \sigma_{xz}, \sigma_{xy}\right)$ is the stress field, and the symbol "T" means matrix transpose. AEWI attempts to invert for the model properties by minimizing the differences between observed seismic data d_{obs} and synthetic data d. To reduce the uncertainties caused by unknown source wavelet, imperfect receiver coupling, etc., we employ a correlative misfit function:

$$\chi(m) = \sum_{N_S N_R}\left[1 - \frac{d_{obs}}{\sqrt{\int_0^t |d_{obs}|^2\, dt}}\frac{d(m)}{\sqrt{\int_0^t |d(m)|^2\, dt}}\right], \tag{3}$$

where N_S and N_R are the numbers of sources and receivers in the monitoring/imaging system, respectively. The gradients of the parameters C_{ij} are calculated using the zero time-lag cross-correlation between the forward propagated source wavefields with the back-propagated adjoint wavefields. For instance, the gradient of the misfit function with respect to the elastic constant C_{11} is given by (Vigh et al., 2014)

$$\frac{\partial \chi}{\partial C_{11}} = -\sum_{N_S N_R}\int_0^t \varepsilon_{11}\varepsilon_{11}^{\dagger} dt, \tag{4}$$

where ε_{ij} and $\varepsilon_{ij}^{\dagger}$ are the forward and adjoint strain fields, respectively. The strain fields can be calculated by combining the elastic compliance and the stress fields based on the Hooke's law. The gradients of the misfit function with respect to other parameters can be derived following the same rule. During inversion, we use the velocity model parameterization to provide improved flexibility and convergence of the inversion. The corresponding gradients can be derived using the chain rule of differentiation. For instance, the gradient for P-wave velocity V_P is given by

$$\frac{\partial \chi}{\partial V_P} = \sum_{i,j}\frac{\partial \chi}{\partial C_{ij}}\frac{\partial C_{ij}}{\partial V_P}. \tag{5}$$

During inversion, we use different step lengths to update different physical parameters to reduce the interparameter trade-offs.

The source and receiver distributions in the ML-CASSM acquisition surveys are sparse. To reduce inversion artifacts and improve the inversion robustness of sparse data, we develop a total generalized p-variation regularization scheme for AEWI using the following misfit function:

$$\chi_{TGPV}(m) = \chi(m) + \alpha_1 \|\nabla m - w\|_p + \alpha_2 \|\varphi(w)\|_p, \tag{6}$$

where φ is a mixed matrix term for holding the second-order spatial derivatives of auxiliary variable w, p is the norm that controls the sparsity-promoting degree, α_1 and α_2 are the regularization parameters. The inverse problem is solved with the alternating direction method of multipliers framework.

2.2 Anisotropic Least-Squares Reverse-Time Migration in Acoustic Media

Because of the sparse acquisition geometry in ML-CASSM, we employ anisotropic, acoustic least-squares reverse-time migration (LSRTM) with modified total-variation regularization to obtain a high-resolution image of CASSM data. The misfit function of the method is given by:

$$J(m) = \frac{1}{2}\|Lm - d_{obs}\|^2 + \lambda_1 \|m - u\|^2 + \lambda_2 \|u\|_{TV}, \tag{7}$$

where L is the Born modeling operator, $\lambda_1 \|m-u\|^2$ and $\lambda_2 \|u\|_{TV}$ are the Tikhonov and total-variation regularization terms, respectively, and λ_1 and λ_2 are the corresponding regularization parameters.

3. APPLICATIONS OF AEWI AND LSRTM TO CASSM DATA FROM EGS COLLAB EXPERIMENT I

3.1 The ML-CASSM Acquisition System

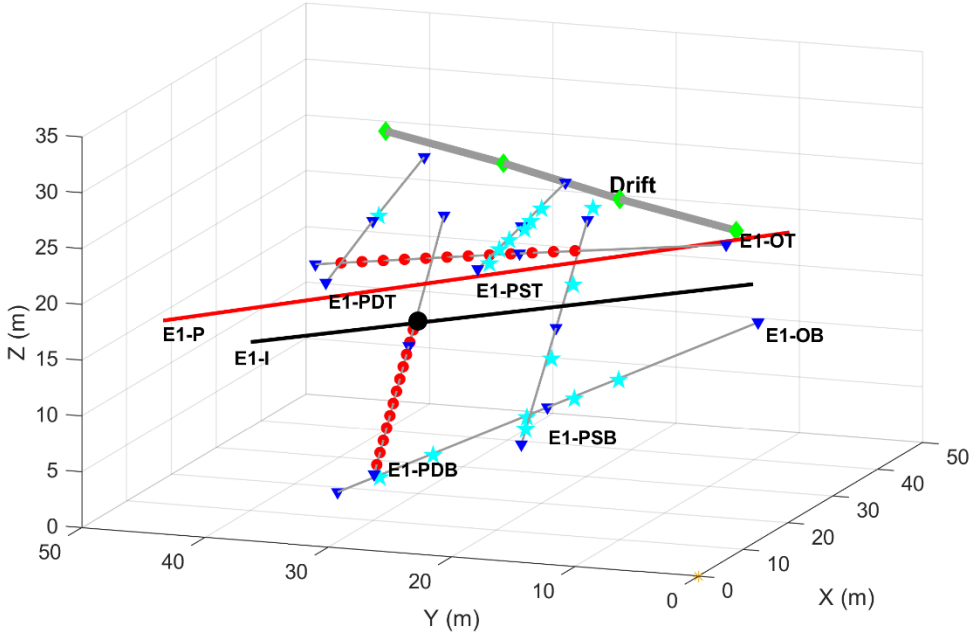

Figure 1: The ML-CASSM acquisition system. The red dots, blue triangles and green diamonds denote the locations of hydrophones, accelerometers and geophones, respectively. The cyan stars indicate the locations of CASSM sources. The black and red lines denote the injection and production wells, respectively. The black dot is the position of the notch at 164.4 ft depth.

Figure 1 shows the schematic illustration of the EGS Collab experiment and ML-CASSM configuration at SURF. Six monitoring boreholes including two shallow fracture-parallel boreholes (E1-PSB and E1-PST), two deep fracture-parallel boreholes (E1-PDB and E1-PDT) and two fracture-orthogonal boreholes (E1-OT and E1-OB), were instrumented. Sixteen CASSM sources (cyan stars) were deployed in the monitoring boreholes. Two strings of 12 hydrophones (HTI-96-Min) spaced 1.75 m and 18 3-C piezoelectric accelerometers (PCB 356B18) were also deployed in the monitoring boreholes, as indicated by the red dots and blue triangles in Figure 1. Another four 3-C geophones (green diamonds) were distributed in sub-vertical jackleg-drilled holes.

In Experiment 1, stimulation tests were carried out on a series of notched locations by injecting fluid from the injection well (E1-I). The notch at 164 ft depth was stimulated several times for fracture creation and extension. On 05/22/2018, the first stimulation lasted about 10.5 minutes at pressures of 23.1 to 25.5 MPa (3350 to 3700 psi) with a total injection volume of 2.1 liters and an injection rate of approximately 200 ml/min, which created one 1.5-m radius fracture. On 05/23/2018, in the second stimulation, more fluid was injected for extending the fracture size. On 05/24/2018, the fracture was extended to intersect with the boreholes of E1-OT and E1-P.

3.2 ML-CASSM Data Analysis

During the hydraulic stimulations, CASSM data were recorded with a maximum time of 0.5 s and a sampling interval of 20.8 μs. Useful data lie in the frequency band of [5 kHz, 25 kHz]. We use the data recorded on 05/24/2018 for seismic inversion and imaging to detect the created fractures. Figure 2 shows the CASSM data recorded by hydrophone string 1 (12 channels) and accelerometers (54 channels) at 22:29:16 on 05/24/2018. The fracture was extended to intersect with E1-OT and E1-P at 22:44 and 22:45 on 05/24/2018 approximately. Figure 3 shows the CASSM data recorded by hydrophone string 1 and accelerometers at 22:47:47 on 05/24/2018 after the fracture creation. Figure 4 shows the corresponding data differences, which are used to image the created fracture.

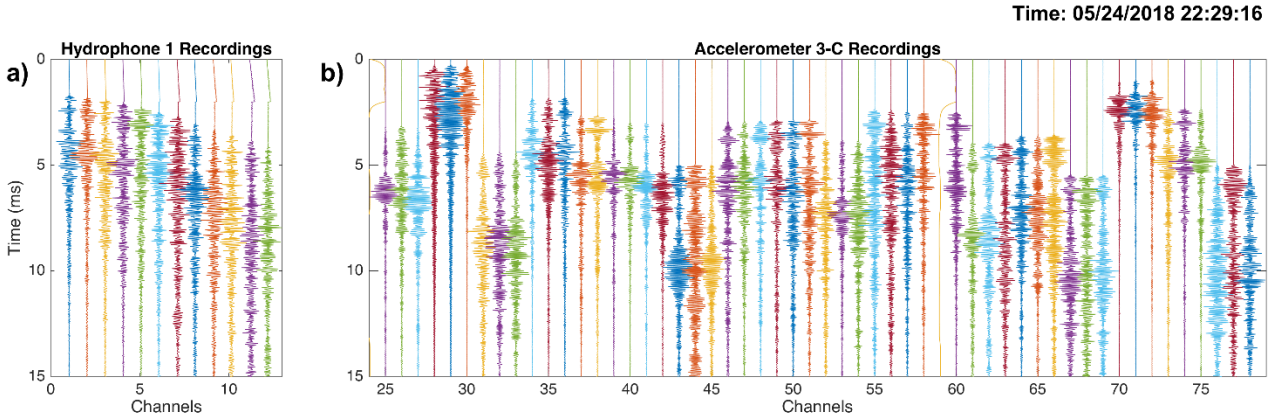

Figure 2: CASSM data recoded by hydrophone string 1 (a) and the 3-C accelerometers (b) at 22:29:16 on 05/24/2018.

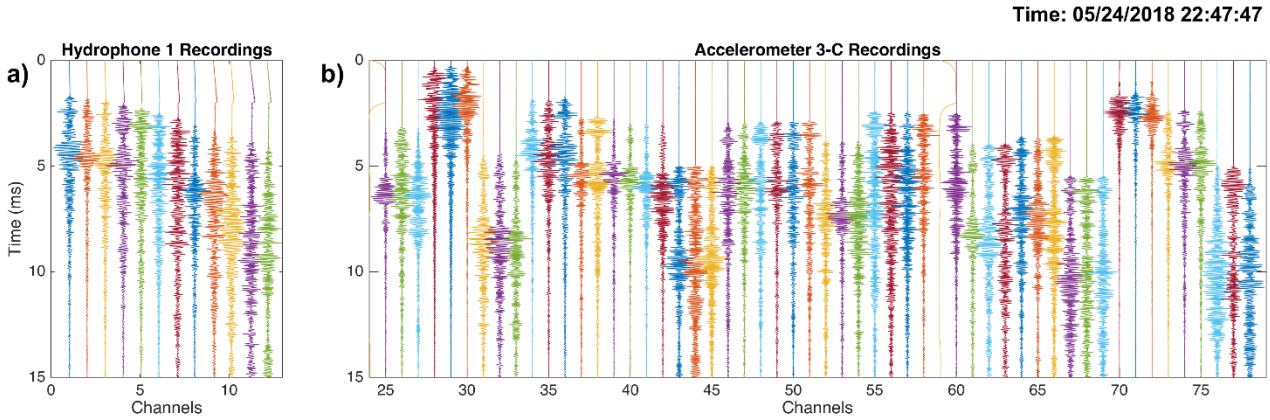

Figure 3: CASSM data recoded by hydrophone string 1 (a) and the 3-C accelerometers (b) at 22:47:47 on 05/24/2018.

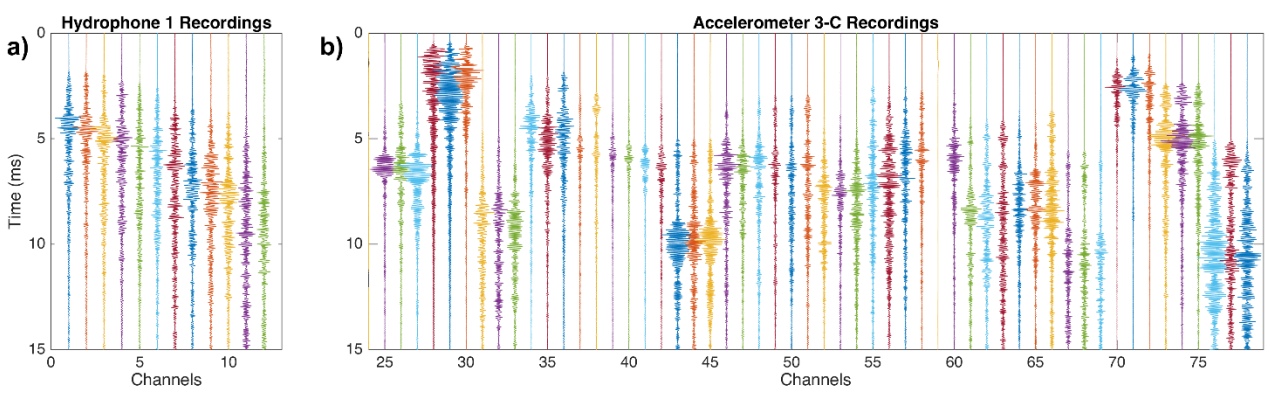

Figure 4: The differences between the CASSM data recorded at 22:29:16 and 22:47:47 on 05/24/2018 by hydrophone string 1 (a) and the 3-C accelerometers (b).

3.3 Results

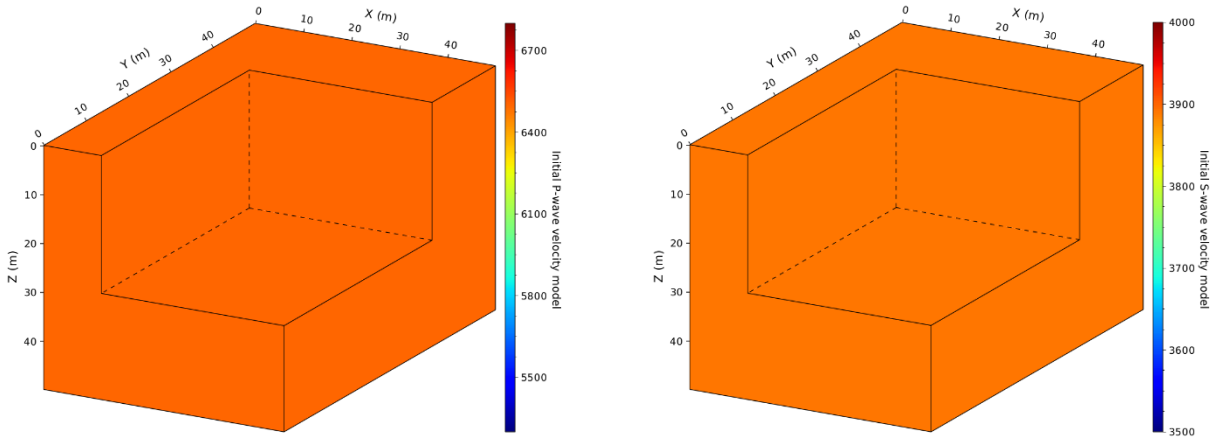

Figure 5: Left: The initial P-wave velocity model with a constant value of 6700 m/s; Right: The initial S-wave velocity model with a constant value of 3950 m/s.

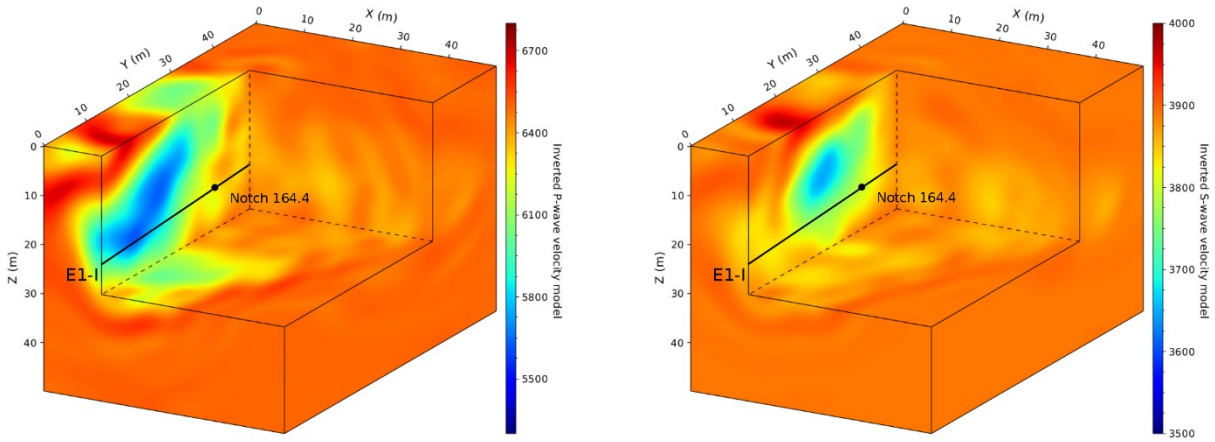

Figure 6: The inverted P-wave velocity model (left) and S-wave velocity model (right) obtained using anisotropic elastic-waveform inversion. The black line indicates the location of injection well E1-I. The black dot denotes the location of the notch at 164.4 ft depth.

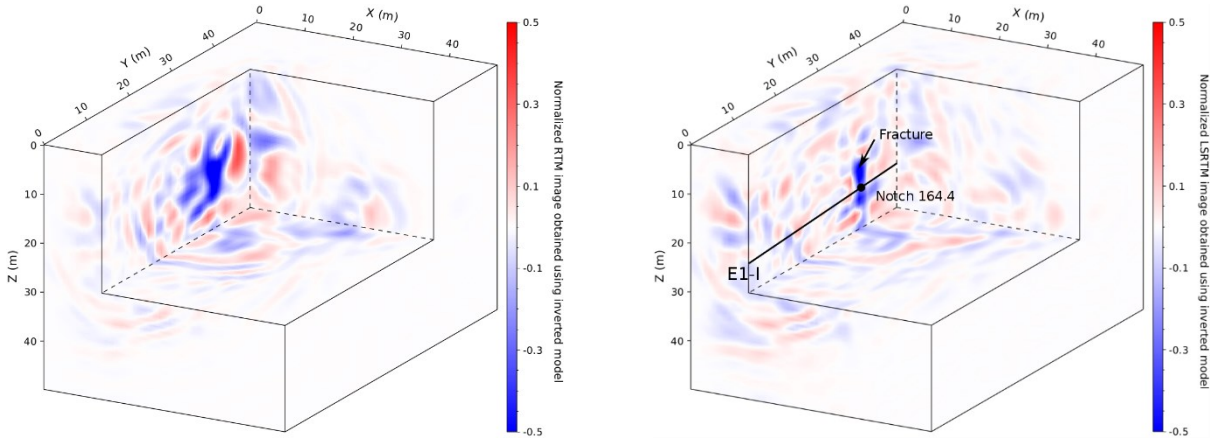

Figure 7: Left: The RTM PP image obtained using the initial velocity models; Right: The LSRTM PP image obtained using the inverted velocity models.

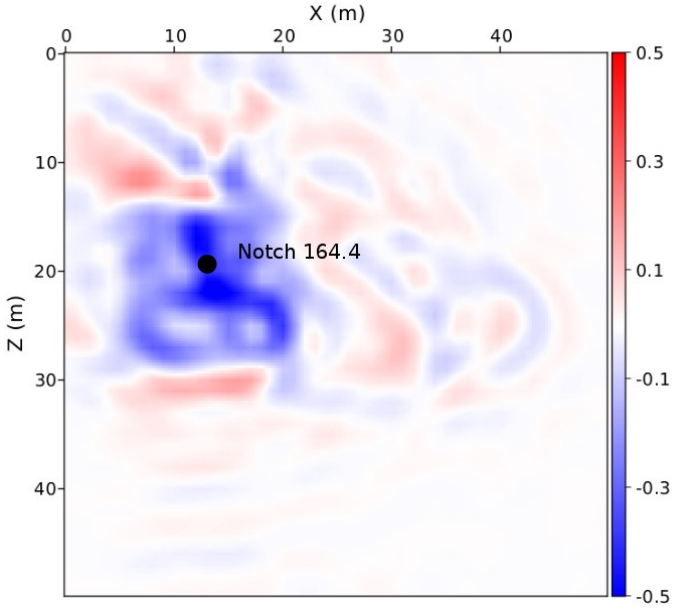

Figure 8: The extracted 2D LSRTM PP image along the fracture plane at Y=27 m.

The initial P-wave velocity and S-wave velocity models are homogeneous with constant values of 6700 m/s and 3950 m/s, respectively, as shown in Figure 5. We apply AEWI to the CASSM data to obtain the velocity models as shown in Figure 6. The inverted models contain low-velocity zones, demonstrating the rock is not homogeneous.

The RTM PP image obtained using the initial velocity models is blurred and noisy, as depicted in left panel of Figure 7. It is difficult to identify the created fracture from this panel. We apply anisotropic, acoustic LSRTM to the CASSM data using the inverted P-wave velocity model, and obtain a high-resolution image as shown in the right panel of Figure 7. The LSRTM PP image clearly show the created fracture as indicated by the arrow. The created fracture intersects with the injection well and match the location of the notch at 164.4 ft depth, which is consistent with the measured location of the notch in the experiments. We extract a 2D LSRTM image along the fracture plane at Y=27 m, as shown in Figure 8, indicating that the created fracture may not be isotropic.

4. CONCLUSIONS

We have conducted 3D anisotropic elastic-waveform inversion of the CASSM data acquired during the Experiment I of the EGS Collab project, and obtained preliminary, improved inversion velocity models for the region of the EGS Collab Experiment I. We have performed anisotropic, acoustic least-squares reverse-time migration of the CASSM data using the inverted velocity models for imaging the created fracture. Our imaging result shows the fracture created by hydraulic stimulation II and some other possible existing fractures. The image of the created fracture intersects perpendicularly with the injection well and matches the location of the notch at 164.4ft depth. We anticipate that anisotropic, elastic least-squares reverse-time migration of the CASSM data can produce an S-wave image with a higher resolution than the PP or P-wave image.

5. ACKNOWLEDGEMENTS

This material was based upon work supported by the U.S. Department of Energy, Office of Energy Efficiency and Renewable Energy (EERE), Office of Technology Development, Geothermal Technologies Office, under Award Number DE-AC52-06NA25396 to Los Alamos National Laboratory (LANL) and Award Number DE-AC02-05CH11231 with Lawrence Berkeley National Laboratory (LBNL). The United States Government retains, and the publisher, by accepting the article for publication, acknowledges that the United States Government retains a non-exclusive, paid-up, irrevocable, worldwide license to publish or reproduce the published form of this manuscript, or allow others to do so, for United States Government purposes. This research used resources provided by the Los Alamos National Laboratory Institutional Computing Program, which is supported by the U.S. Department of Energy National Nuclear Security Administration under Contract No. 89233218CNA000001.

REFERENCES

Ajo-Franklin, J.B., Daley, T.M., Butler-Veytia, B., Peterson, J., Wu, Y., Kelley, B., and Hubbard, S.: Multi-level continuous active source seismic monitoring (ML-CASSM): Mapping shallow hydrofracture evolution at a TCE contaminated site, *Extended Abstracts of Society of Exploration Geophysicists Annual Meeting*, (2011).

Gao, K., Huang, L., Chi, B., Ajo-Franklin, J., & EGS Collab Team. (2018). Imaging Fracture Zones Using Continuous Active Source Seismic Monitoring for the EGS Collab Project: A Synthetic Study. In *Proceedings 43th Workshop on Geothermal Reservoir Engineering, Stanford University.*

Kneafsey, T. J., Blankenship, D., Knox, H. A., Johnson, T. C., Ajo-Franklin, J., Schwering, P. C. and, … EGS Collab Team. (2019). *EGS Collab Project: Status and Progress. In Proceedings 44th Workshop on Geothermal Reservoir Engineering, Stanford University*.

Vigh, D., Jiao, K., Watts, D., and Sun, D., (2014), Elastic full-waveform inversion application using multicomponent measurements of seismic data collection. *Geophysics*, 79 (2), R63-R77.